

## Generalized two-temperature model for coupled phonons

Meng An<sup>1,2,#</sup>, Qichen Song<sup>1,2,#,†</sup>, Xiaoxiang Yu<sup>1,2</sup>, Zelin Jin<sup>1,2</sup>, Dengke Ma<sup>1,2</sup>, Baoling Huang<sup>3,4</sup>, and Nuo Yang<sup>1,2\*</sup>

<sup>1</sup>State Key Laboratory of Coal Combustion, Huazhong University of Science and Technology, Wuhan 430074, People's Republic of China

<sup>2</sup>Nano Interface Center for Energy (NICE), School of Energy and Power Engineering, Huazhong University of Science and Technology (HUST), Wuhan 430074, People's Republic of China

<sup>3</sup>Department of Mechanical and Aerospace Engineering, The Hong Kong University of Science and Technology, Clear Water Bay, Kowloon, Hong Kong

<sup>4</sup>The Hong Kong University of Science and Technology Shenzhen Research Institute, Shenzhen, 518057, China

# M.A. and Q.S. contributed equally to this work.

† Current address: Department of Mechanical Engineering, Massachusetts Institute of Technology, 77 Massachusetts Avenue, Cambridge, MA 02139, USA.

\* To whom correspondence should be addressed. E-mail: (N.Y.) [nuo@hust.edu.cn](mailto:nuo@hust.edu.cn)

## Abstract

The design of graphene-based composite with high thermal conductivity requires a comprehensive understanding of phonon coupling in graphene. We extended the two-temperature model to coupled phonons driven by the gradients of temperature fields. These equations identify some new physical quantities, the phonon-phonon coupling factor and length, to characterize the phonon coupling quantitatively. Besides, our proposed coupling length has an obvious dependence on system size. These studies would provide a brand new strategy in enhancing thermal conductivity of graphene-based composites and deepen our understanding of phonon transport in the emerging two-dimensional materials.

**KEYWORDS:** Phonons, TTM, coupling strength, graphene, molecular dynamics simulations

## Introduction

Multi-carrier interactions such as electron-phonon<sup>1-5</sup> and phonon-magnon<sup>6</sup>, play a crucial role in thermal management and conversion. A major issue in heat transfer and thermal management is how to understand and describe phonon-phonon (ph-ph) coupling<sup>7</sup>, especially in semiconductors and insulators where phonons dominate. Unlike scattering of different phonon eigen-modes from the view of anharmonic lattice dynamics<sup>8, 9</sup>, the ph-ph coupling between different phonon groups, a collection of interactions, is a brand new perspective to shed light on the phonon interactions.

The ph-ph coupling between different phonon groups affects the design strategy of graphene-based thermal nanocomposites<sup>10, 11</sup> significantly. Recently, some reports show that there two effects largely contributing to low interfacial thermal conductance between graphene and matrix materials<sup>11</sup>. One is the poor coupling between the group of high-frequency in-plane phonons and the group of low-frequency out-of-plane phonons in a graphene sheet. The other one is that the steady state between the two groups is not established. However, how to quantitatively characterize the coupling of graphene between different phonon groups has not yet been realized but is rather imperative and interesting.

The two-temperature model (TTM) has been successfully applied to investigate the coupling between different energy carriers in thermal nonequilibrium<sup>6, 12</sup>. For example, several authors have generalized TTM for the coupled phonon-magnon diffusion and predicted a new magnon cooling effect<sup>6</sup>. In TTM, different energy carriers are considered as two interacting subsystems. Besides, some reports show TTM is implemented with molecular dynamics (TTM-MD) to

include all ph-ph interactions at any order of anharmonicity and is used to study electron-phonon coupled thermal transport in metal/semiconductor systems<sup>13, 14</sup>.

Here, we extended TTM to investigate the coupling between different phonon groups. This method is demonstrated on graphene, a representative two-dimensional material with the highest known thermal conductivity<sup>15, 16</sup>. We separate phonons in graphene into two groups, namely in-plane (IP) and out-of-plane (OP) phonon group. Based on the temperature profiles of different phonon groups, we calculated the ph-ph coupling factor  $G_{io}$ , comparable with strength of electron-phonon coupling<sup>14</sup> and found that  $G_{io}$  is not sensitive to system size. We successfully demonstrated the poor coupling between IP and OP phonon groups in graphene<sup>17-20</sup>. The most interesting finding is the ph-ph coupling length we proposed can potentially provide some guidance for designing graphene-based thermal composites. These investigations are beneficial for understanding the thermal transport in low-dimensional materials.

## Theoretical analysis

In this letter, TTM is used to investigate the ph-ph coupling between OP and IP phonon groups. As shown in the configuration (Figure 1), the entire system is divided into two regions, namely, the left region (*l*) (where atoms have both OP and IP vibrations) and the right region (*r*) (only IP vibration).  $T_H$  ( $T_C$ ) is the prescribed temperature of hot (cold) bath at the left (right) end. As observed in the left region, the temperature difference between OP and IP phonon groups increases and reaches a maximum value,  $\theta_{max}$ , at the interface. This phenomenon results from the distinguishing thermal transport capability and the poor coupling between OP and IP phonon groups, which is a necessary condition for validity of TTM<sup>6, 13</sup>.

Similar to the electron-phonon coupling<sup>1, 13</sup>, the governing equations for coupled phonon transport (considering a simple one-dimensional situation) states,

$$\kappa_o \frac{d^2 T_o}{dx^2} = G_{io} (T_o - T_i) \quad (1a)$$

$$-\kappa_i \frac{d^2 T_i}{dx^2} = G_{io} (T_o - T_i) \quad (1b)$$

where  $\kappa_o$  and  $\kappa_i$  are the thermal conductivity of IP and OP phonon groups, respectively.  $T_o$  and  $T_i$  are the temperature of OP and IP phonon groups, respectively.  $G_{io}$  is the ph-ph coupling factor and denotes the local energy exchange rate between OP and IP phonon groups.

Subtracting Eq. (1a) from Eq. (1b), we can obtain  $d^2\theta/dx^2 - \gamma^2\theta = 0$ , where  $\theta = T_o - T_i$  and  $\gamma = \sqrt{G_{io}(1/\kappa_i + 1/\kappa_o)}$ . Based on the boundary condition  $\theta|_{x \rightarrow -\infty} = 0$  and  $\theta|_{x=0} = \theta_{\max}$ , the temperature difference profile is written as  $\theta = \theta_{\max} \exp(\gamma x)$ .

Here, we propose the ph-ph coupling length,  $l_c$ , shown in Figure 1, to quantitatively characterize the coupling between them. Its physical meaning is the distance required to equilibrate OP and IP phonon groups when the temperature difference exists. Specifically, we define such a characteristic length as the distance between the position of  $\theta_{\max}$  and  $5\%\theta_{\max}$ :

$$l_c = \frac{-\ln(5\%)}{\gamma} \approx \frac{3}{\gamma} = \frac{3}{\sqrt{G_{io} \left( \frac{1}{\kappa_i} + \frac{1}{\kappa_o} \right)}} \quad (2)$$

## Numerical Simulations

The ph-ph coupling length of graphene is numerically calculated by means of TTM-MD, and the detailed non-equilibrium MD simulation setup is shown in Figure 2(a). The heat source with a higher temperature  $T_H=310\text{K}$  is applied to the atoms in red region and the heat sink with a lower temperature  $T_C=290\text{K}$  is applied to atoms in blue region where only IP phonons exist. All of our simulations are performed by large-scale atomic/molecular massively parallel simulator (LAMMPS) packages<sup>21</sup>. The fixed (periodic) boundary conditions are used along the x (y) direction. The optimized Tersoff potential<sup>22</sup> is applied to describe interatomic interactions, which has successfully reproduced the thermal transport properties of graphene<sup>23, 24</sup>. The velocity Verlet algorithm is adopted to integrate the discrete differential equations of motions. The time step is set as 0.5fs. We relaxed the graphene structure in the isothermal-isobaric (NPT) ensemble. After NPT relaxation, simulations are performed for 2ns to reach a steady state. After that, a time average of the temperature and heat current is performed for 10ns.

The thermal conductivity is calculated based on the Fourier's Law<sup>25</sup>  $\kappa = -J/A \cdot \nabla T$ , where  $J$  denotes the heat current transported from the hot bath to cold bath,  $A$  is the cross section area and  $\nabla T$  is the temperature gradient along the x direction. The temperature of different phonon

groups is computed by  $T_p(x) = \langle \sum_{i=1}^N m_i \overset{\rightarrow}{v}_{i,p} \cdot \overset{\rightarrow}{v}_{i,p} \rangle / (Nk_B)$ , where  $\overset{\rightarrow}{v}_{i,p}$  is the velocity vector of phonon vibrating along  $p$  direction, i.e. IP or OP, of atom  $i$ .  $N$  and  $k_B$  are the number of atoms in the simulation cell and the Boltzmann constant, respectively. Besides, it is calculated that the thermal conductivity of IP (OP) including only the atomic vibration along in-plane (out-of-plane) direction by freezing the other direction. The simulations detail is shown in Supplementary Information (SI).

## Results and Discussion

In our simulations, the width of simulation cell is set as 5.2 nm. The lattice constant ( $a$ ) and thickness ( $d$ ) of graphene are 0.143 nm and 0.335 nm, respectively. The size effect could arise if the width is not sufficiently large<sup>26, 27</sup>. The thermal conductivity reaches a saturated value when the width is larger than 5.2 nm which is consistent with our previous works<sup>27, 28</sup>. Besides, to examine the accuracy of MD results we calculated thermal conductivity ( $\kappa$ ) of suspended single-layer graphene with a length ( $L$ ) as 33 nm. The calculated  $\kappa$  is  $1082 \pm 103$  W/m-K, which is consistent with previous studies<sup>23, 24</sup>.

The temperature profile of TTM-MD is presented in Figure 2(b), where the system length along x direction is 101 nm. In the left region, there are obvious differences between the temperature curves of IP and OP phonons. It is found that the maximum temperature difference ( $\theta_{\max}$ ) is 5.1 K at the interface. In order to extract the ph-ph coupling length ( $l_c$ ), the profile of  $\theta$  in Figure 2(c) is fitted exponentially, based on theoretical solution of Eq. (1). Then,  $l_c$  can be obtained based on its definition as the distance between the position of  $\theta_{\max}$  and  $5\% \theta_{\max}$ . If the system length is not large enough to equilibrate different phonon groups, the coupling length would be larger than system length. That is IP and OP subsystems are under inequilibrium state. We calculated four simulation cells with different length, and  $l_c$  are 60 nm, 64 nm, 70 nm and 77 nm corresponding to length is 33 nm, 60 nm, 67 nm, and 101 nm, respectively. The profiles of temperature difference with  $L=33$ nm, 67nm, 70nm is shown in Supplementary Information (SI).

To evaluate the ph-ph coupling factor ( $G_{io}$ ) based on Eq. (2), we calculated the thermal conductivity of IP/OP phonon groups ( $\kappa_i/\kappa_o$ ) including only the atomic vibration along in-plane (out-of-plane) direction (shown in Figure 3(a)). It is also shown that the summation of  $\kappa_i$  and

$\kappa_o$  approximately equals to the thermal conductivity of single-layer suspended graphene (blue solid sphere), instead of an obvious reduction by scatterings. This phenomenon in graphene arises from the poor ph-ph coupling between OP and IP<sup>18, 20, 29</sup> and the decoupled phonon scattering interaction between OP and IP of freezing method<sup>20</sup>.

In low dimensional nanostructures, the thermal conductivity becomes dependent on the characteristic length of system due to the length is comparable to phonon mean free path (MFP)<sup>30</sup>. However, the controversy exists on how the thermal conductivity of graphene is dependent on the system size. Some works<sup>28, 31</sup> argued that  $1/\kappa$  is proportional to  $1/L$  when the system size is comparable with and smaller than the MFP of phonons that dominate thermal transport. On the other hand, recent experimental studies<sup>15</sup> showed that the thermal conductivity of graphene increases logarithmically ( $\sim \log L$ ) with the size of sample. The emphasis in our studies is not the size dependence of thermal conductivity of graphene. Therefore, both the two size dependences of thermal conductivity are taken to fit MD results shown in Fig. 3(a-b).

With the  $\kappa_i$ ,  $\kappa_o$  and  $l_c$  for several systems with different lengths, we can calculate the ph-ph coupling factor  $G_{io}$  based on Eq. (2). To the best of our knowledge, it is the first time to extract the ph-ph coupling factor. It is found that  $G_{io}$  in graphene is not sensitive to system length, and the average value is  $4.26 \times 10^{17} \text{ W/m}^3\text{-K}$ , which is comparable with the electron phonon coupling factor ( $G_{ep}$ ) in metals ranging from  $5.5 \times 10^{16} \text{ W/m}^3\text{-K}$  to  $2.6 \times 10^{17} \text{ W/m}^3\text{-K}$ <sup>14</sup>.

As shown in Figure 4(b), we obtained the size dependence of ph-ph coupling length of graphene based on the size dependence of the thermal conductivity. It is clearly observed that the ph-ph coupling length shows two behaviors due to the two different size dependence of thermal conductivity. The value of  $l_c$  converges to 77.5 nm when assuming  $1/\kappa \sim 1/L^{26}$ . While,  $l_c$  diverges when  $\kappa \sim \log L^{15}$ . Combining with the definition of  $l_c$  in Eq. (4), it is easy to understand that the size dependence of thermal conductivity contributes to the size effect of  $l_c$ .

The ph-ph coupling factor and length may provide us a new way in understanding heat transfer. For example, the weak coupling means there are less scatterings between IP and OP phonons, which attribute to the ultra-high high thermal conductivity in suspended graphene sheet. The coupling factor and length provide a way in explanation quantitatively. On the other side, we recall that the poor thermal performance of graphene-based composites, which is corresponding to the interfacial thermal resistance (named as outer resistance)<sup>10, 11</sup>. Besides, the longer ph-ph coupling length means it is difficult to reach the equilibrium state between IP and OP phonons corresponding to a larger inside thermal resistance. Based on the discussion above, the thermal conductivity of graphene-based composite could be enhanced by using the size of graphene nanoparticles larger than coupling lengths.

## Conclusion

In summary, we have extended the TTM to investigate the coupled phonon implemented with molecular dynamics. The merit of this work lies in the fact that we applied the techniques widely used in the field of electron-phonon interactions to investigate the ph-ph interactions, utilized the analogy between field-driven electron and phonon, and combined IP and OP

phonon groups in a smooth way. The magnitude of ph-ph coupling factor has been estimated in graphene and is independent of system size. Besides, we proposed the ph-ph coupling length associated with the ph-ph coupling strength. These investigations can not only deepen our understanding of thermal transport in two-dimensional materials, but provide a brand new perspective in designing graphene-based composites with high thermal conductivity.

## Acknowledgements

This project is supported by the National Natural Science Foundation of China (Grant 51576076). We are grateful to Shiqian Hu for useful discussions. The authors thank the National Supercomputing Center in Tianjin (NSCC-TJ) and China Scientific Computing Grid (ScGrid) for providing assistance in computations.

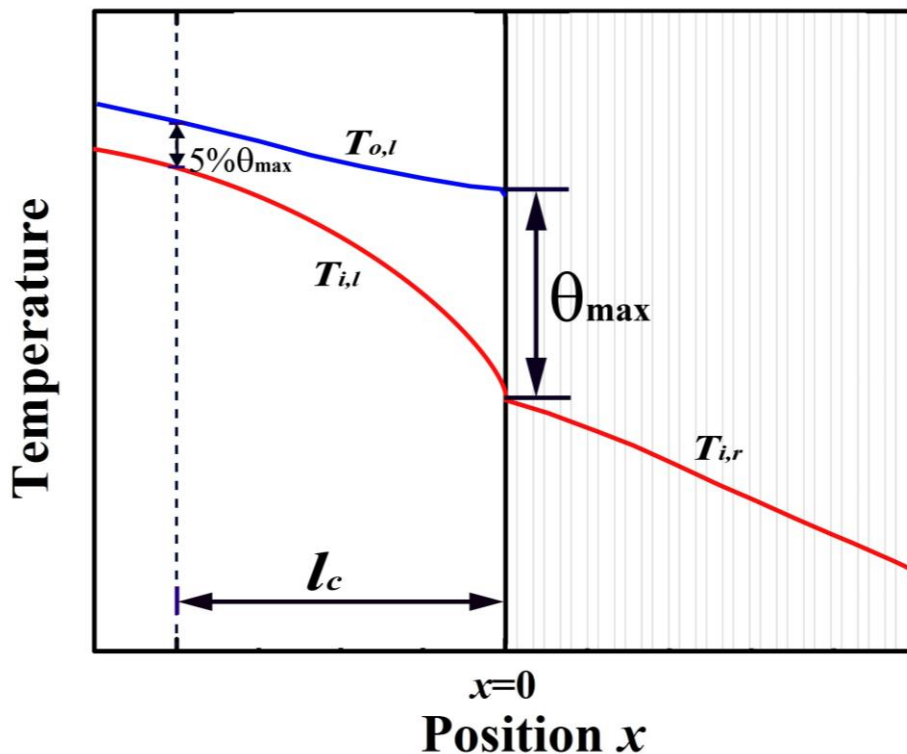


**Figure 1** (Color on-line) Representative temperature profiles in TTM for the coupled phonon.

The system consists of two regions, namely, the left region (*l*) (where atoms have both OP and IP vibrations) and the right region (*r*) (only IP vibration).  $T_{o,l}$ ,  $T_{i,l}$  are temperatures for OP and IP phonon group in the left region.  $T_{i,r}$  is the temperature of IP phonon group in the right region.  $\theta_{max}$  is the maximum temperature difference between OP and IP phonon group.  $l_c$  is the ph-ph coupling length, which is defined as the distance between the position of  $\theta_{max}$  and  $5\%\theta_{max}$ .

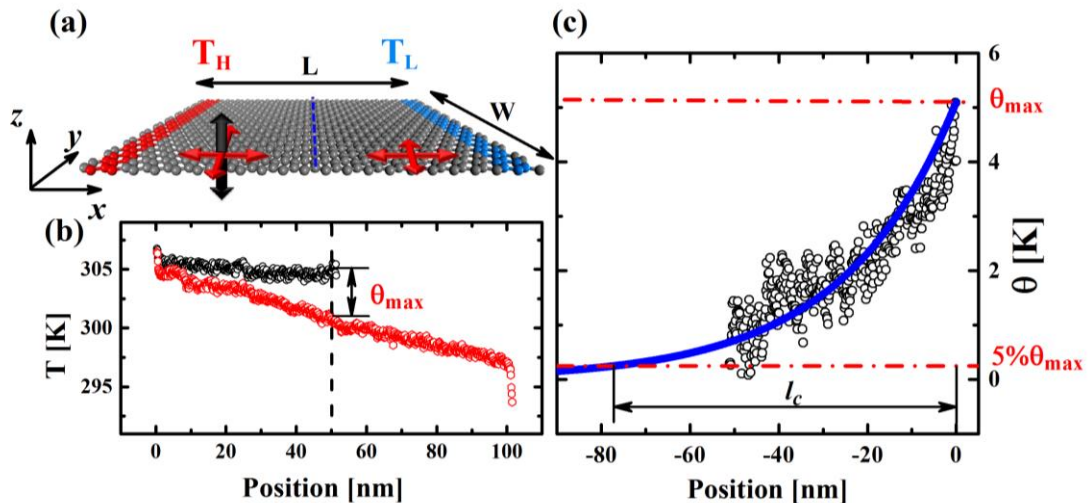


Figure 2 (Color on-line) (a) Schematic illustration of molecular dynamics simulation setup. The black (red) arrow denotes the vibration along the out-of-plane (in-plane) direction. The blue dot line is the interface of different simulation regions. The atoms in the left region vibrate freely in three directions while those in the right region could only vibrate along in-plane direction. The fixed (periodic) boundary condition is applied to along  $x$  ( $y$ ) direction. Hot bath (red atoms)  $T_H$  and cold bath (blue atoms)  $T_C$  are applied. The temperatures of two heat baths are set as  $T_H=310\text{K}$ ,  $T_C=290\text{K}$ , respectively. (b) The temperature profile of different phonon groups. (c) The temperature difference distribution between OP and IP phonon group when the system length is set as  $L=101\text{nm}$ . The fitting line is based on  $\theta=\theta_{\max} \exp(\gamma x)$ . The red dot lines denote the maximum temperature difference and its five percent, respectively.

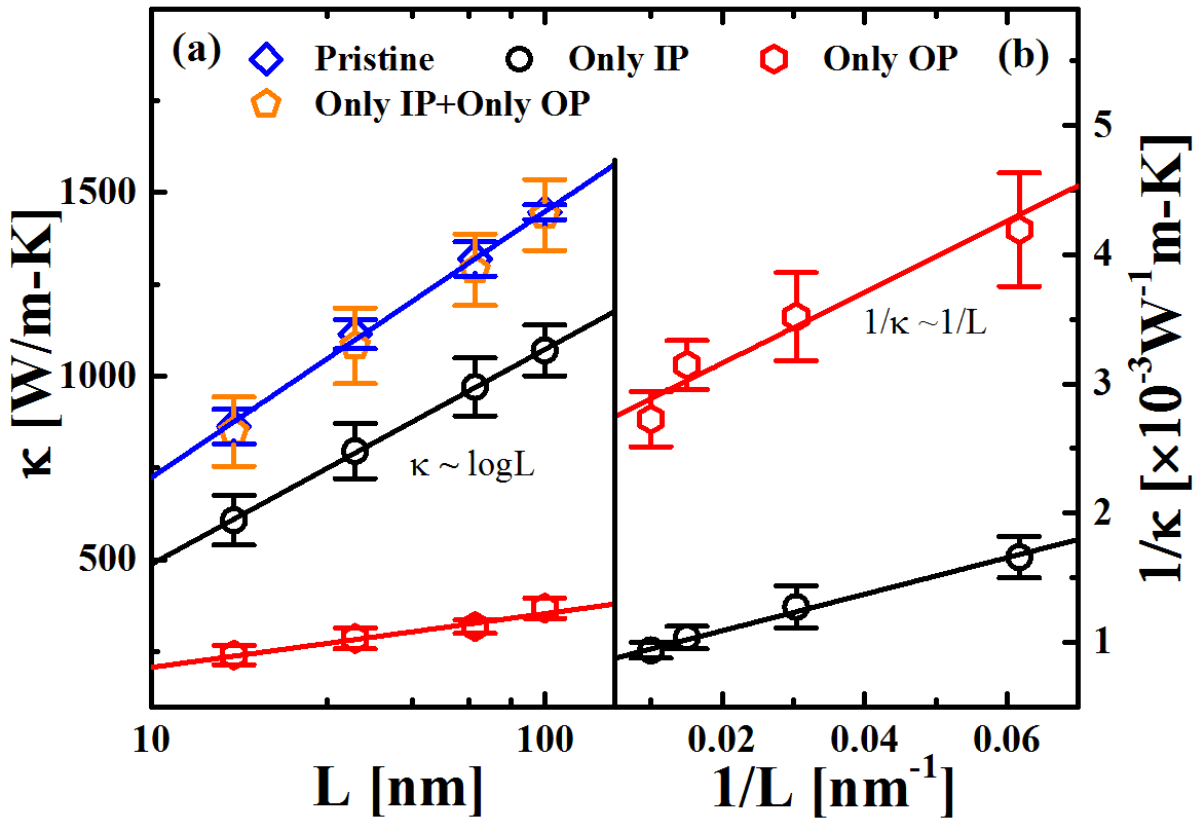


Figure 3. (Color on-line) The length dependence of thermal conductivity with different phonon groups in graphene calculated from NEMD. (a) Blue open diamond (Pristine graphene), Black open circles (Only IP), red open hexagon (only OP), Orange open pentagon (the summation of only IP and only OP). The system length ranges from 16nm to 100nm. The fitting lines in the left figure are based on  $\kappa \sim \log L$ , which has been demonstrated by the experimental measurements<sup>15</sup>. (b) The fitting lines in the right figure are based on the  $1/\kappa \sim 1/L$ .

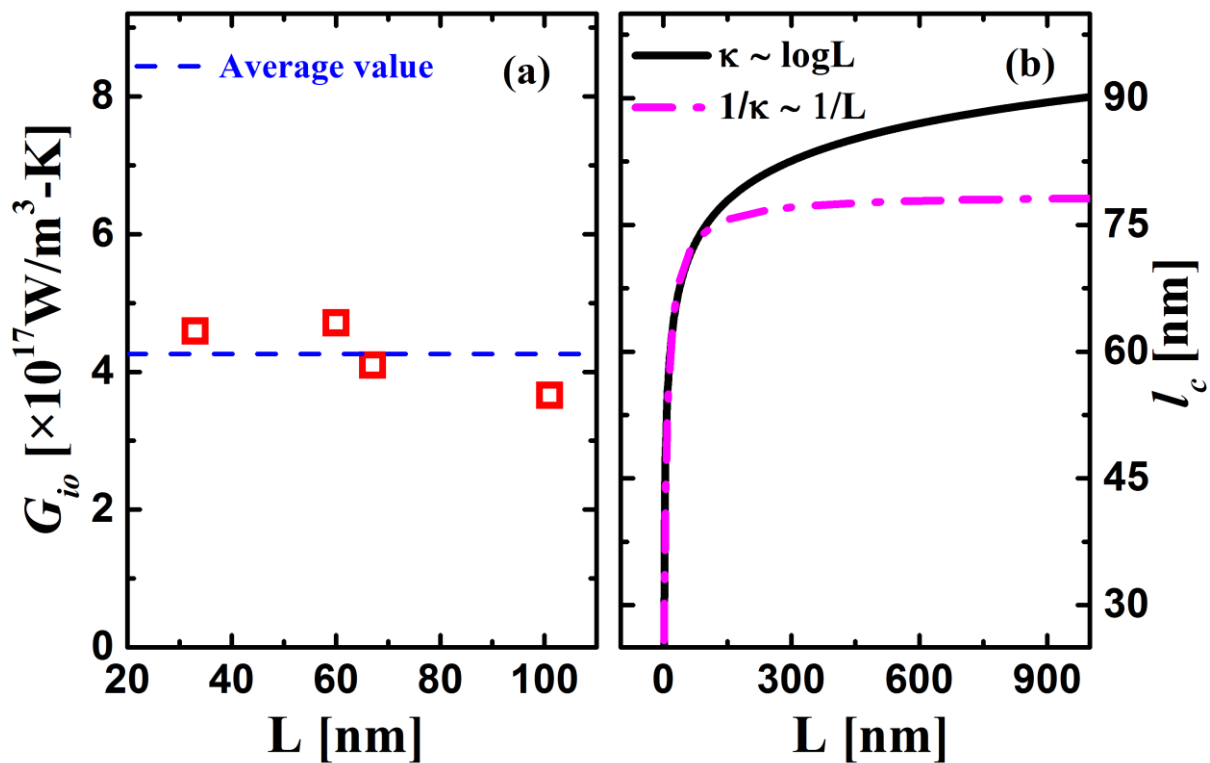


Figure 4. (Color on-line) (a) The ph-ph coupling factor versus the system lengths. (b) The length dependence of the ph-ph coupling length. The thermal conductivity of graphene is fitted with  $\kappa \sim \log L$  (black solid line) and  $1/\kappa \sim 1/L$  (magenta dash line), respectively.

## References

1. Majumdar, A.; Reddy, P. *Appl. Phys. Lett.* **2004**, 84, (23), 4768-4770.
2. Liao, B.; Qiu, B.; Zhou, J.; Huberman, S.; Esfarjani, K.; Chen, G. *Phys. Rev. Lett.* **2015**, 114, (11).
3. Liao, B.; Zhou, J.; Qiu, B.; Dresselhaus, M. S.; Chen, G. *Phys. Rev. B* **2015**, 91, (23).
4. Liao, B.; Maznev, A. A.; Nelson, K. A.; Chen, G. *Nat. Commun.* **2016**, 7, 13174.
5. Vallabhaneni, A. K.; Singh, D.; Bao, H.; Murthy, J.; Ruan, X. *Phys. Rev. B* **2016**, 93, (12).
6. Liao, B.; Zhou, J.; Chen, G. *Phys. Rev. Lett.* **2014**, 113, (2).
7. Cepellotti, A.; Marzari, N. *Phys. Rev. X* **2016**, 6, (4), 041013.
8. Maradudin, A. A.; Fein, A. E. *Phys. Rev.* **1962**, 128, (6), 2589-2608.
9. Maradudin, A. A.; Fein, A. E.; Vineyard, G. H. *physica status solidi (b)* **1962**, 2, (11), 1479-1492.
10. Hu, L.; Desai, T.; Keblinski, P. *Phys. Rev. B* **2011**, 83, (19), 195423.
11. Liu, Y.; Huang, J.; Yang, B.; Sumpter, B. G.; Qiao, R. *Carbon* **2014**, 75, 169-177.
12. Majumdar, A.; Reddy, P. *Appl. Phys. Lett.* **2004**, 84, (23), 4768.
13. Wang, Y.; Ruan, X.; Roy, A. K. *Phys. Rev. B* **2012**, 85, (20).
14. Lu, Z.; Wang, Y.; Ruan, X. *Phys. Rev. B* **2016**, 93, (6).
15. Xu, X.; Pereira, L. F.; Wang, Y.; Wu, J.; Zhang, K.; Zhao, X.; Bae, S.; Tinh Bui, C.; Xie, R.; Thong, J. T.; Hong, B. H.; Loh, K. P.; Donadio, D.; Li, B.; Ozyilmaz, B. *Nat Commun* **2014**, 5, 3689.
16. Balandin, A. A.; Ghosh, S.; Bao, W.; Calizo, I.; Teweldebrhan, D.; Miao, F.; Lau, C. N. *Nano Lett.* **2008**, 8, (3), 902-7.
17. Zhang, J.; Wang, Y.; Wang, X. *Nanoscale* **2013**, 5, (23), 11598-603.
18. Zhang, J.; Wang, X.; Xie, H. *Phys. Lett. A* **2013**, 377, (41), 2970-2978.
19. Zhang, J.; Huang, X.; Yue, Y.; Wang, J.; Wang, X. *Phys. Rev. B* **2011**, 84, (23).
20. Zhang, H.; Lee, G.; Cho, K. *Phys. Rev. B* **2011**, 84, (11).
21. Plimpton, S. *J. Comput. Phys.* **1995**, 117, (1), 1-19.
22. Lindsay, L.; Broido, D. A. *Phys. Rev. B* **2010**, 81, (20).
23. Yang, L.; Chen, J.; Yang, N.; Li, B. *Int. J. Heat Mass Transfer* **2015**, 91, 428-432.
24. Chen, J.; Zhang, G.; Li, B. *Nanoscale* **2013**, 5, (2), 532-6.
25. Yang, N.; Zhang, G.; Li, B. *Nano Lett.* **2008**, 8, (1), 276-280.
26. Schelling, P. K.; Phillpot, S. R.; Keblinski, P. *Phys. Rev. B* **2002**, 65, (14).
27. Shiqian, H.; Meng, A.; Nuo, Y.; Baowen, L. *Nanotechnology* **2016**, 27, (26), 265702.

28. Song, Q.; An, M.; Chen, X.; Peng, Z.; Zang, J.; Yang, N. *Nanoscale* **2016**, 8, (32), 14943-9.
29. Zhang, J.; Wang, X.; Xie, H. *Phys. Lett. A* **2013**, 377, (9), 721-726.
30. Yang, N.; Xu, X.; Zhang, G.; Li, B. *AIP Advances* **2012**, 2, (4), 041410.
31. Hong, Y.; Zhang, J.; Huang, X.; Zeng, X. C. *Nanoscale* **2015**, 7, (44), 18716-24.